IEEE Access
Multidisciplinary | Rapid Review | Open Access Journal

Received 13 December 2023, accepted 7 February 2024, date of publication 19 February 2024, date of current version 23 February 2024.

Digital Object Identifier 10.1109/ACCESS.2024.3366998

RESEARCH ARTICLE

Multi-UAV Coverage Path Assignment Algorithm Considering Flight Time and Energy Consumption

YANG YU AND SANGHWAN LEE
Department of Computer Science, Kookmin University, Seoul 02707, South Korea

Corresponding author: Sanghwan Lee (sanghwan@kookmin.ac.kr)

This work was supported in part by the Global Scholarship Program for Foreign Graduate Students at Kookmin University, South Korea; in part by the Basic Science Research Program through the National Research Foundation of Korea (NRF) funded by the Ministry of Education under Grant 2022R1F1A1074672; and in part by the Ministry of Food and Drug Safety under Grant 22183MFDS436.

ABSTRACT Coverage path planning is an important research direction for unmanned aerial vehicles (UAV), which are primarily used in ground search or mapping scenarios. Although there have been a large number of studies on UAV coverage path planning, there are still some problems in the cooperative work of multi-UAV in complex environments under the constraints of energy consumption and work efficiency requirements of UAV. To solve unnecessary energy loss when multiple UAVs jointly execute complex area coverage tasks and improve the overall work efficiency of the UAV swarm. In this study, we simulated the situation of multiple UAVs performing the mission of area coverage under the constraints of the corresponding energy consumption in a work environment with no-fly zones. We propose the use of multiple UAV base stations to provide takeoff and landing services for UAVs that perform missions. We proposed two algorithms. One is the multi-base station multi-UAV cooperative coverage path planning algorithm with flexible obstacle avoidance ability (MBS-MUCCPPAFOA), which performs coverage route planning from an entire area using multiple base stations to perform multi-UAV area coverage tasks. The other algorithm is a multi-UAV cooperative coverage path planning algorithm with flexible obstacle avoidance capability based on area segmentation (MUAV-CCPPAFOA-AS), which divides the entire work area and performs coverage path planning for each sub-area to perform multi-UAV area coverage tasks. We compared the proposed algorithm with the common scanning coverage path planning algorithm, and proved the robustness of the proposed MBS-MUCCPPAFOA and MUAV-CCPPAFOA-AS algorithms.

INDEX TERMS Cooperative unmanned aerial vehicle teams, coverage path planning problems, CPP, path planning, multiple traveling salesmen problems, MTSP, predictive task assignment, task allocation, unmanned aerial vehicles, UAV.

I. INTRODUCTION

With the development of artificial intelligence and remote sensing technology, UAV technology is becoming increasingly mature, and its reliability, convenience, and practicality are greatly enhanced. With the gradual opening of low-altitude airspace, UAVs can play more roles and become increasingly critical. UAVs play an increasingly important role in ground surveillance and have been widely used in multiple scenarios [1], such as cargo delivery [2], damage assessment [3], [4], mapping [5], [6], crop growth collection [7], [8], and personnel search and rescue [9].

When the UAV completes the aforementioned tasks, it must fly along a specific path, which involves a path planning issue. Route planning of UAV can be separated into two groups based on various planning requirements and objectives: path planning to accomplish the beginning point to the endpoint [10] and path planning to achieve regional coverage [11]. Path planning from the starting point to the endpoint is mostly applied to UAV delivery, UAV

The associate editor coordinating the review of this manuscript and approving it for publication was M. Anwar Hossain.

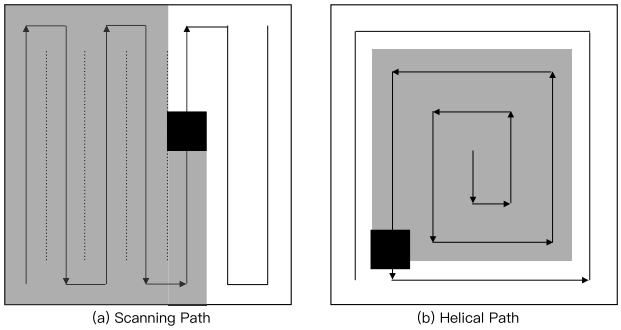

FIGURE 1. Unobstructed area coverage path.

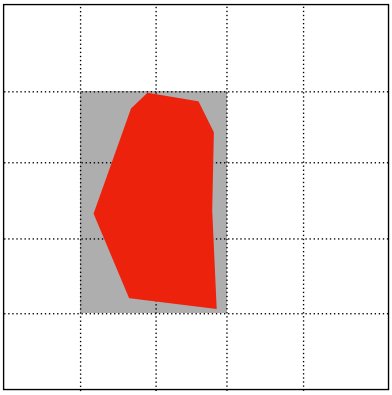

FIGURE 2. Example of domain decomposition (cell decomposition).

near-ground strikes, and route modification of civil aviation aircraft [12]. In these problems, the UAV has a definite starting point and ending point and only needs to consider the obstacles between the two points and adopt certain methods to generate the path, and its technology is relatively mature. In contrast to path planning from the starting point to the endpoint, path planning aimed at regional reconnaissance coverage must consider more constraints and deal with global information. In the case of zone accessibility, simple actions are usually required to meet the coverage needs. One of the most common coverage methods is the reciprocating path method, as shown in Fig. 1(a), which is simple and guarantees complete coverage. Another common method is the spiral path [13], as shown in Fig. 1(b), which starts from the central point of the region and extends outwards along the spiral line.

When there are obstacles or no-fly zones in the target area in addition to the barrier-free area, it is necessary to divide it from the barrier-free area, that is, area decomposition. Reference [14] first proposed a grid-based method for decomposing the working domain into a uniform set of grid cells. Each grid cell uses a value that indicates whether an obstacle exists at the corresponding location. This value can be binary or probabilistic. Each grid cell can be square, triangular, or hexagonal. Methods such as grid partitioning are also classified as cell decomposition methods because they are spatially uniform. Fig. 2 shows an example of a cell decomposition. Domain decomposition decomposes the entire working area into simple, non-overlapping sub-regions. The union of all sub-regions fills the available space. These sub-regions without obstacles can be covered by UAV with simple actions. Areas with obstacles must be bypassed. Methods involving domain decomposition generate the covering paths in two steps. First, the space is decomposed, and the result is organized in the form of an adjacency graph. The most important method for domain decomposition is to determine the covering order of the domain. Coverage path planning requires avoiding all obstacles in a given target area and planning a continuous and uninterrupted UAV flight path covering all points in the environment [15]. After the UAV completes the flight by the planned path, it can traverse the target area and complete related tasks such as regional target reconnaissance, hazard monitoring, and map construction [16], [17], [18].

Path planning and task cooperation are two key issues for a UAV swarm to perform coverage path planning (CPP) tasks. UAV swarm path planning is usually defined as a function optimization problem under complex constraints. By solving the optimal solution or sub-optimal solution of the objective function, an optimal or sub-optimal path from the starting point to the goal point is found for each UAV. The path needs to satisfy the characteristics of high computational efficiency and low cost of UAV flight. Task cooperation is the basis for ensuring that the UAV swarm completes a task. Usually, an overall task is decomposed into multiple sub-tasks, which are then assigned to each UAV. Task cooperation requires that each UAV can work together to complete the specified overall task while satisfying complex conditions and the shortest flight distance. In previous studies, the task allocation problem of a UAV swarm was usually transformed into integer programming and assignment problems, multiple traveling salesman problems, and vehicle routing problems. These problem transformation schemes can provide certain references and inspiration for our CPP task in Multi-UAV. In a real scene, it is often necessary to search and scan multiple discrete areas distributed over a wide range of areas, and it is not feasible to rely solely on drones with limited endurance. The vehicle is used as the loading base station for multiple UAVs, and the mode of cooperation between the vehicle and multiple UAVs can significantly expand the effective scanning radius. The collaborative mode of vehicle-mounted UAV was first proposed in [19]. In the area scanning task, the vehicle needs to carry multiple UAVs close to the target area and select a suitable parking point to release and recover the UAV. This approach can significantly reduce the drone's working time and improve the efficiency of the mission. In this study, we plan the deployment location of the base stations for UAVs to improve their overall efficiency.

OUR CONTRIBUTION

In this study, we focus on the path planning problem for multiple UAV coverage in a working area with a no-fly area and the corresponding solution algorithm. The main results of this study can be summarized as follows:

- The simulation environment was clearly defined, and the UAV swarm coverage path planning problem was transformed into a function optimization problem under complex constraints. Aiming at the proposed work area coverage search problem with a no-fly zone, the previously proposed Multi-UAV cooperative search algorithm was improved.
- We propose a new coverage path optimization method, that adds multiple UAV departure base stations to the work area, uses different base stations as the main departure base stations, plans the coverage path of the work area, and selects the optimal coverage path.
- We propose two heuristics to satisfy the full coverage search of the working area from the overall and regional segmentation perspectives.

The remainder of the paper is organized as follows: In Section II, we describe the research background of this study and related research work on Multi-UAVs. In Section III, we propose several heuristic multi-UAV cooperative search algorithms that are mainly used to improve the collaborative work efficiency of multiple UAVs. In Section IV we present the results of our evaluation and analysis of the proposed algorithm. Section V concludes the paper.

II. LITERATURE REVIEW

In this section, we discuss the related advantages of Multi-UAV coverage path planning review the existing techniques on UAV coverage path planning, and discuss the remaining problems.

Because the entire effort is dispersed, deploying many UAVs can considerably shorten task completion. Many UAVs studies offer advantages in coverage path planning [20]. The use of multiple UAVs can improve the robustness of the entire UAV system, and the failure of some UAVs can be compensated for by other UAVs. Cluster intelligence algorithms have been widely used in multi-coverage path planning problems; for example, [21] improves the distributed ant colony algorithm and proposed an intelligent self-organization algorithm for the collaborative search task of multiple UAVs. Each UAV is given the ability to make autonomous decisions, and the algorithm is highly real-time, flexible, and reliable; however, it has too many limitations in practical applications. A swarm of UAVs was used in [22] to conduct an online search in an uncharted area. This method can guarantee the broadest possible coverage in an emergency; however, it cannot ensure total coverage. Therefore, academics focus more on work allocation-based methodologies. These techniques expand the coverage route planning method for a single UAV to several UAVs by employing specific tactics to distribute duty burden. The work area can be divided into several sub-areas according to the initial position of the UAV or the percentage of the search area for each UAV, which allows each UAV to search its sub-area and select the appropriate route to reduce the redundancy of the search path. This method focuses on the coverage of the UAV in a single cell and the allocation method of the UAV among cells. Task allocation can provide ideas for our research.

Many researchers have studied cooperative search coverage algorithms for UAVs. Some existing approaches for UAV environment coverage and partition optimization are summarized below. The planning algorithm based on the spiral spanning tree proposed in [23] reduced the traversal overlap, but the number of planned path turns increased, resulting in a longer path distance. Reference [15] proposed that a full coverage path can be obtained by cell decomposition [24], which reduces the difficulty of planning. However, the decomposition method, establishment of the adjacency graph, and selection of full coverage of sub-regions need to be further considered. Aiming at the low coverage rate of the sub-regions, [25] proposes full coverage planning based on the backtracking method, which has the advantages of high operation efficiency and low repetition rate, but it is difficult to establish this backtracking mechanism. In [26], an improved potential field grid algorithm was proposed by combining the grid method and the distance conversion method, which solved the problem of the high computational complexity of the path; however, the effect of the planned path in the large working area was poor and the coverage rate was low. Reference [27] proposed a full coverage path planning method based on the grid method, which can prevent the robot from falling into a dead zone and can effectively avoid obstacles; however, the algorithm is complex and requires a large amount of calculation.

Scanning and spiral routes are the two primary types of routes used in the conventional full-coverage path planning method. Although the route is straightforward and quick to execute, there are issues such as path redundancy and poor coverage. Therefore, the Multi-UAV cooperative search coverage path planning algorithm proposed in this paper is based on the MUCS-BSAE (Multi-UAV Cooperative Search Algorithm Based on Binary Search Algorithm with Energy) algorithm [28]. By confirming the unit position of the no-fly area in the work area where the original planned route is located, and then using the four-domain A* algorithm sub-region for secondary planning, the coverage path of the sub-region is obtained, and the adjacent path is established, to complete the planning path of the entire work area.

III. MULTI-UAV COVERAGE PATH PLANNING PROBLEMS AND ALGORITHMS

In this section, we define the environment of the coverage path planning problem. We specify the goal of our algorithm, which is to satisfy the requirement of covering the entire working area and minimizing the work time, and then detail the heuristics we propose separately.

TASK SCENARIO DESCRIPTION

In a previous study [28], we used the ''square wave signal'' path to perform distributed scanning of the open working area

for multiple UAV groups. However, in real situations, there are often no-fly areas for obstacles in the scanning area, and the UAV must avoid them according to the actual situation. Furthermore, in an actual UAV search-coverage mission, the environment is very complex. To establish a quantifiable mathematical model, it is necessary to abstract and simplify an environmental model. We ignored the flying altitude of the UAV and used an onboard camera sensor to search and detect the environment and targets. The camera sensor detects the ground, as shown in Fig. 3. Therefore, the search area in this study does not consider the height information, and it is assumed to be a two-dimensional planar graph. Therefore, based on our previous research, we simulated a target area with obstacles or no-fly areas. The working area is typically rectangular in practical UAV search coverage operations; therefore, we define the working area as a rectangular area with length L and width W. Different UAVs are equipped with different onboard camera sensors, so the radius of the area that can be detected by the camera sensor is also different. We define the radius that the camera sensor can detect as R, and the area that the camera sensor can see is a square with side length $D = 2R$. We used the unit area that the camera sensor can detect as a grid to decompose the entire working area into cells. To maximize the coverage of the entire rectangular working area, when the length L and width W of the area cannot be divided by D integers, they are assigned according to the following formula:

$$m = \begin{cases} L//D, & X \bmod D = 0 \\ L//D + 1, & \text{otherwise} \end{cases}$$
$$n = \begin{cases} W//D, & X \bmod D = 0 \\ W//D + 1, & \text{otherwise} \end{cases} \quad (1)$$

The work area can be divided into a grid of $m * n$ dimensions. The cell in the grid row i and column j is designated as (i, j). Consequently, the center position of cell (i, j) is $C_{i,j} = (i \times D + R, j \times D + R)$. We define the working region as *SPACE* and use one-hot encoding to represent the state of the cell region in *SPACE*. We use numerical mapping for different cell states: when a cell is not the UAV is explored and when there are no obstacles within the cell, the cell state $C_{state}$is identified as 0. When there is an obstacle in the cell, the current cell-cell state $C_{state}$is identified as 2. If a cell identified as 0 is explored by the drone, the cell state $C_{state}$of that cell is converted to 1. The rest of the aircraft does not scan the cell again when it passes through the cell. We can express the state of every cell in this target region as an $m \times n$ dimensional matrix as follows:

$$SPACE(x, y) \rightarrow \begin{bmatrix} C_{\text{state }(0,n-1)} & C_{\text{state }(1,n-1)} & \cdots & C_{\text{state }(m-1,n-1)} \\ \vdots & & \vdots & \vdots \\ C_{\text{state }(0,1)} & C_{\text{state }(1,1)} & \cdots & C_{\text{state }(m-1,1)} \\ C_{\text{state }(0,0)} & C_{\text{state }(1,0)} & \cdots & C_{\text{state }(m-1,0)} \end{bmatrix} \quad (2)$$

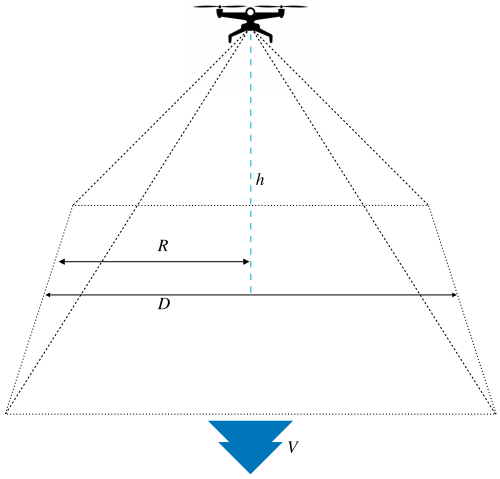

FIGURE 3. Illustration of the UAV search.

In *SPACES*, the number 1 represents the cell that has been explored and the number 2 represents the cell with an obstacle, and the number 0 represents a cell that has not yet been scanned. Here's an example:

$$SPACES \rightarrow \begin{bmatrix} 1, & 1, & 1, & 1, & 1, & 1, & 1, & 1, & 1, & 1 \\ 0, & 0, & 0, & 0, & 0, & 0, & 0, & 0, & 0, & 0 \\ 0, & 0, & 0, & 0, & 0, & 2, & 2, & 2, & 0, & 0 \\ 0, & 0, & 0, & 0, & 0, & 0, & 0, & 0, & 0, & 0 \\ 0, & 0, & 0, & 0, & 0, & 0, & 0, & 0, & 0, & 0 \\ 0, & 0, & 0, & 0, & 0, & 0, & 0, & 0, & 0, & 0 \\ 0, & 0, & 0, & 0, & 0, & 0, & 0, & 0, & 0, & 0 \\ 0, & 0, & 0, & 0, & 0, & 0, & 0, & 0, & 0, & 0 \end{bmatrix} \quad (3)$$

THE BASIC PATH OF COVERAGE PATH PLANNING

In our previous study [28], we designed five UAV flight paths: (1) Snake curve path, (2) "Square wave signal" curve path, (3) Piano curve path, (4) Hilbert curve path, and (5) Moore curve path. By comparing the simulation results, we found that the 'square wave signal" curve path is a near-optimal path to the other flight paths.

So in this study, we adopt the "Square wave signal" curve path as our basic path. Here, we briefly introduce the "Square wave signal" curve path. The work area is divided by the cell area, which can appear as odd or even numbered columns in two cases. When divided into even columns, the UAV enters the nearest cell region from starting position S. It first moves to the leftmost cell area of the spatial area, moves in the form of a "square wave signal", and then completes the cell area coverage search task in the row closest to the UAV departure base station and returns to the starting position S. When dividing the odd sequence, the procedure is the same as the even column, but when the UAV reaches the penultimate column opposite to the starting position, the UAV will make a "square wave signal" shape move to the side close to the starting position. The unmanned vehicle reaches the cell area in the row closest to the departure base station of the UAV

TABLE 1. Simulation parameters.

Parameter	Value	Unit
$SPACE$: Status coding for each cellular region within the working area	$0, 1, 2$	-
N: The number of the dromes	-	-
R: The radius that the camera sensor can detect	$\in [10, 50]$	m
D: The side length of the unit square of the decomposed cell and is also the diameter detected by the camera sensor	$\in [20, 100]$	m
S: Coordinates of the takeoff position of the UAV (Base station position coordinates)	-	-
$SrcList$: A collection of base station location coordinates	$[S_0, ..., S_3]$	-
P: List of flight path coordinates of the drone based on the "square wave signal" curve path	$[P_0, P_1, \ldots, P_{mn-1}]$	-
$\hat{P}$: List of flight path coordinates of the drone based on the "square wave signal" curve path	$[\hat{P}_0, \hat{P}_1, \hat{P}_2, ..., \hat{P}_x]$	-
HT: The hovering time of the UAV for each cell	1	s
V: The flying speed of the UAV	5, 10, 15, 20	m/s
SEL: Percentage of energy consumed per second by UAV at corresponding speeds	0.110, 0.135, 0.210, 0.300	%
$HTEL$: Percentage of energy lost per second while hovering	0.0757	%

with a step length D, completes the detection task in the last part, and returns to the starting position S, as shown in Fig. 4. The "square wave signal" curve path planning path is denoted as $P = [P_0, P_1, \ldots, P_{mn-1}]$, and the ith cell under the "square wave signal" path rule is P_i.

Because several UAVs cover a work area, they work together to jointly complete the task of covering it. UAVs are all information collectors because they perform the same functions. The entire environment can be divided, and each UAV is given a responsibility area, to make the work of each UAV more apparent and to limit the behavior dependence between the aircraft. Each aircraft conducts the partition coverage task and plans the coverage path for its defined partition. Controlling this situation depends on how effectively the entire area can perform a coverage task. If the assigned workload is unbalanced (the size of the division is varied) for a set of aircrafts with the same capability, the coverage period of various partitions will vary. Therefore, temporal consistency, which is merely used as a trajectory constraint for the flight path of our proposed Multi-UAV cooperative coverage path planning algorithm is not necessary. It is possible that the working time is not synchronized when the UAVs in the formation work together to fulfill the coverage task in a particular area. The operating time of the last drone returning to the base station is used as the operating time of the swarm. We define some parameter values in Tab 1.

OBSTACLE AVOIDANCE RULES FOR PATH

We adopt the "Square Wave Signal" curve path as our base path. The UAV carries out coverage search work in the work area where there is a no-fly zone or obstacle. The UAV flight roadbed needs to make the UAV avoid the obstacle or no-fly zone and bypass the obstacle or no-fly zone to the next cell area that can be reached with in the shortest possible time. The traditional four-domain A* algorithm was used. Four-domain A* can avoid obstacles more effectively than eight-domain A*. In Fig. 5, the black solid line represents the path, the blue arrow solid lines represent the planned path, the black arrow dotted line represents the shortest path of obstacle avoidance, and the red areas are unable to reach areas.

In UAV path planning, if the original path cannot reach the next cell area in $P_{current}$, the original path searches for the P_{target} that can be reached. The shortest path from $P_{current}$ to P_{target} was calculated as a new path according to the A* algorithm. The shortest path from $P_{current}$ to P_{target} is calculated according to the A* algorithm as a new path to replace the no-fly area or cell area where the obstacle is located.

Therefore, the flight path $\hat{P}$ of the UAV in the working area with obstacles or no-fly areas is different from the number of cell areas passed by the original flight path P of the UAV based on the "Square Wave Signal" curve path planning. The path of the UAV is denoted as $\hat{P} = [\hat{P}_0, \hat{P}_1, \hat{P}_2, \ldots, \hat{P}_x]$. $\hat{P}_i$ denotes the îth cell on the path, and $dist(\hat{P}_i - \hat{P}_{i+1})$ denotes the Euclidean distance between the two points.

We set the overall maximum working time *Maxtime* as the time when one UAV can completely explore all the cell areas in the coverage area without an energy consumption limitation. We define the moving speed of the UAV as V, the UAV starts the scanning task from the starting point with the speed V, and every time it reaches a cell region with state 0, it hovers for HT seconds to scan the cell region and take photos. We define T_1 is defined as the time required for the UAV to move from starting point S to the first target cell area. If the $\hat{P}_0$ cell state is 1, the UAV moves to the $\hat{P}_0$ cell area but does not hover to scan and capture photos. The time consumed by the UAV was $\frac{dist(\hat{P}_0 - S)}{v}$. If the state of $\hat{P}_0$ cell is 0, the UAV needs to hover for HT seconds to capture a picture and scan the cell. The consumed time $\frac{dist(\hat{P}_0 - S)}{v} + t$, from cell i to cell $i+1$ is expressed as follows:

$$T_{i,i+1} = \begin{cases} HT + \dfrac{dist(\hat{P}_{i+1} - \hat{P}_i)}{v} & \text{if } \hat{P}_{i+1} \text{ cell state is 0} \\ \dfrac{dist(\hat{P}_{i+1} - \hat{P}_i)}{v} & \text{if } \hat{P}_{i+1} \text{ cell state is 1} \end{cases} \tag{4}$$

The time taken to return from the last cell to the starting point is represented by $T_{back} = \frac{dist(\hat{P}_x - S)}{v}$. Therefore, the following is the expression of the time consumed by the UAV to complete all cell scanning tasks:

$$Maxtime = T_1 + \sum_{i=1}^{x-2} T_{i,i+1} + T_{back} \tag{5}$$

When assigning a working path to each UAV using path $\hat{P}$ generated by the obstacle avoidance rule as its working

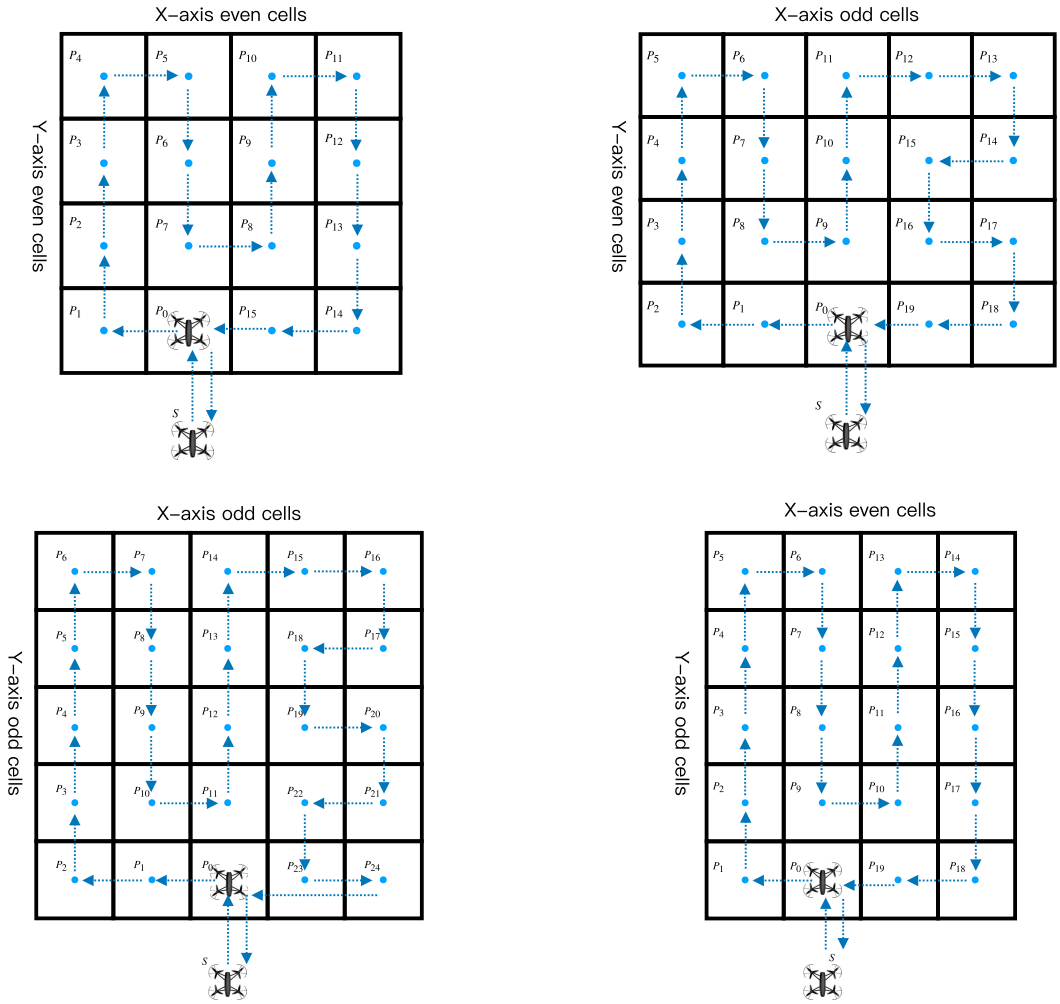

FIGURE 4. "Square wave signal" curve path.

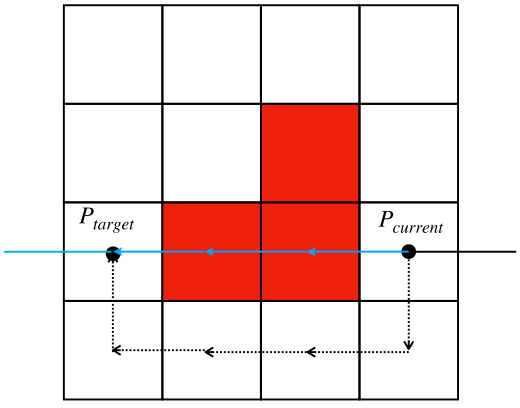

FIGURE 5. A* Algorithm strategies for avoiding obstacles.

path, the previous UAV returns to the starting point S at $\hat{P}_{i-1}$. According to the planning of the working path, the next UAV continues the allocation from $\hat{P}_i$ which causes UAV to carry out unnecessary energy consumption tests. Therefore, to reduce unnecessary energy consumption, the next UAV flies to $\hat{P}_{target}$ from starting point S as shown in Fig 6.

When the UAV avoids obstacles, if the new path contains the cell area inside the working area, the UAV will scan the cell area; if it contains the cell area outside the working area, the UAV will not scan the cell area outside the working area. The process of obstacle avoidance flight allows the cell areas with lower coverage order in the original path P to be covered and searched in advance. To reduce the unnecessary energy loss caused by repeated scanning of the UAV, the UAV will not hover to search these cell areas again. Because the work areas have obstacles, the UAV cannot return to the position of base station S, therefore every cell in the subsequent scans of the area before the UAV was calculated based on the A * algorithm from the next cell area the energy for the position back to base station S.

A. MULTI-UAV COOPERATIVE COVERAGE PATH PLANNING ALGORITHM WITH FLEXIBLE OBSTACLE AVOIDANCE ABILITY

In this section, based on the MUCS-BSAE Algorithm [28], we propose a Multi-UAV cooperative coverage path planning algorithm with flexible obstacle avoidance ability, called

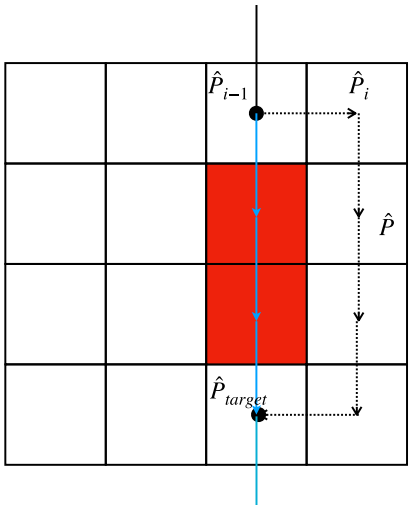

FIGURE 6. Obstacle avoidance strategy.

MUAV-CCPPAFOA. We set the starting position S of the UAV to be directly below the $C_{\text{state }((m-1)//2,0)}$ cell on one side of the overall work area, as shown in Fig. 4. We define the number of UAV as N, the initial energy of the UAV as E, the moving speed of the UAV as V, the energy consumed per second at the current speed V is SEL, the hovering scanning time of the UAV is HT, the energy consumed per second during the hovering scanning is $HTEL$, and the UAV must return to the base station S position when its own energy is insufficient.

Because of the existence of obstacles or no-fly areas in the work area, returning directly from $\hat{P}_i$ to starting position S in a straight line or reaching $\hat{P}_i$ from starting position S in a straight line may pass through the no-fly area or collide with obstacles. Therefore, the UAV must find the path from position $\hat{P}_i$ to starting position S through the A* algorithm to avoid accidents during the return process and stray into the no-fly area. First, we assign each drone work time T, when UAVs from position $\hat{P}_i$ moved to $\hat{P}_{i+1}$, need to be calculated and deducted from $\hat{P}_i$ to $\hat{P}_{i+1}$ moves needed to consume time. Then, according to $\hat{P}_{i+1}$ position state determines whether to hover scan, if $\hat{P}_{i+1}$ position status to 0 to deduct in the position of $\hat{P}_{i+1}$ the time required to hover the scan, if $\hat{P}_{i+1}$ position state to 1 is not required. The time required to return to starting position S from $\hat{P}_{i+1}$ must be calculated and deduced according to the A* algorithm. If the current remaining working time T of the UAV cannot satisfy the above conditions, the UAV immediately returns to starting position S from $\hat{P}_i$. If the rest of the work time satisfies the above conditions, the UAV from $\hat{P}_i$ moved to $\hat{P}_{i+1}$, and deducted from the $\hat{P}_i$ moved to $\hat{P}_{i+1}$ consumed time, and based on the $\hat{P}_{i+1}$ position state, choose whether to deduct the time of the hover scan. We use the binary search algorithm as the basis, and take *Maxtime* as the overall maximum working time of the UAV to assign an appropriate working time T to each UAV and assign an appropriate flight sequence of the cell area. Simultaneously, we calculate whether each UAV

FIGURE 7. MUAV-CCPPAFOA algorithm UAV coverage path assignment example diagram.

can complete the assigned task at a given time T according to the energy consumption. If a UAV has not completed the task, it indicates that the current working time T is too high. The UAV cannot complete the task based on the current energy consumption, and the assigned working time must be reduced. If all the UAVs have been assigned tasks and the UAVs can successfully complete the tasks under the current energy consumption, it proves that the UAVs can successfully complete the assigned tasks under the current energy consumption to ensure that the UAVs can achieve the purpose of the shortest working time of the entire UAV group under the energy consumption. The UAV coverage path assignments are shown in Fig. 7. Pseudocode as in Algo. 1.

B. MULTI-BASE STATION MULTI-UAV COOPERATIVE COVERAGE PATH PLANNING ALGORITHM WITH FLEXIBLE OBSTACLE AVOIDANCE ABILITY

In the study in Section III-A, the UAV flies from the base station location S to a location with a long distance or returns to the base station location S from a location with a long distance, which consumes a lot of energy and time. In view of this situation, we propose a Multi-base station Multi-UAV cooperative coverage path planning algorithm with a flexible obstacle avoidance ability, called MBS-MUCCPPAFOA. This algorithm uses multiple base stations to provide a path assignment scheme for UAVs. We set four fixed base stations, $S = S_0, S_1, S_2, S_3$around the target area to support UAV take-off and return. The four base stations were located at the center of the edge of the target working area. When the UAV performs the search coverage task, it calculates the nearest base station assigned to the current position as the departure and return base stations of the UAV. Let $dist(a, b)$ be the

Algorithm 1 MUAV-CCPPAFOA

Input: $Maxtim$, $\hat{P}$, $SPACE$, V, E, HT, S, SEL, $HTEL$, N
Output: P_{Drones}, t

L ← 0
U ← $Maxtime$
LP_{Drones} ← []
while True **do**
  t ← $\frac{L+U}{2}$
  P_{Drones} ← []
  for $i = 1$ to N **do**
    T_u ← t
    LP ← S
    P_u ← []
    j ← 0
    while True **do**
      C ← $\hat{P}[j]$
      C_{state} Find the state of C in $SPACE$
      t_c ← $\frac{dist(LP,C)}{V}$
      if C_{state} is 0 **then**
        t_c ← $\frac{dist(LP,C)}{V}+HT$
      t_b, $List_b$ //time and path coordinates of C back to S
      if $T_u \geq t_c + t_r$ **then**
        t_u ← $t_u - t_c$
        C_{state} ← 1
        C append to P_u
        LP ← C
      else
        Add the path coordinates of LP back to S to P_u
        break
      j ← $j + 1$
    Remove the travelled point from $\hat{P}$
    $\hat{P}$[: 1] ← path coordinates of S move to C
  if $0 \notin SPACE'$ and $LP_u \geq P_u$ **then**
    U ← t
    LP_u ← P_u
  if $0 \notin SPACE'$ and $LP_u = P_u$ **then**
    if $\forall i \in \{1, 2, \ldots, N\}, \sum_{j=1}^{n} E_{ij} \leq E$ **then**
      break
    U ← t
  if $0 \in SPACE'$ **then**
    L ← t
return P_{Drones}, t

path distance between two points a and b based on the A* algorithm. The base station closest to the current location can be found as follows:

$$n^* = \text{argmin dist}\,(S_n, P_{current}) \tag{6}$$

Similar to the MUAV-CCPPAFOA algorithm, this algorithm must allocate the flight sequence of each UAV's cell area according to the assigned working time T. When assigning a path to the first drone, the drone flies from the starting position S to $\hat{P}_0$, and when the drone needs to move from $\hat{P}_i$ to $\hat{P}_{i+1}$, it is necessary to calculate the time consumed to move from $\hat{P}_i$ to $\hat{P}_{i+1}$ and the time consumed to move to $\hat{P}_{i+1}$ based on the $\hat{P}_{i+1}$ position state to choose whether to deduct the time needed to hover and scan, and to calculate the time consumed to each base station $S = S_0, S_1, S_2, S_3$ while in position $\hat{P}_{i+1}$, and to choose a base station to return with the least amount of time needed to be consumed. If the current remaining working time of the UAV satisfies the above conditions, the UAV moves from $\hat{P}i$ to $\hat{P}_{i+1}$and deducts the corresponding time, and deducts the time needed to hover and scan according to the position state of $\hat{P}_{i+1}$. If the current residual energy or working time of the UAV cannot meet the above conditions, the UAV returns from $\hat{P}_i$to the nearest base station from $\hat{P}_i$. The second UAV then starts from the base station returned by the previous UAV and continues to allocate the remaining exploration tasks, the rest of the UAV, etc. In addition to the MUAV-CCPPAFOA algorithm, binary search technology is used to calculate whether each UAV could complete the assigned task at a given time T according to the energy consumption. If the assigned task cannot be completed, the allocated time T is further reduced. Ensure that the UAV can successfully complete the assigned task under the energy consumption. The different locations of obstacles or no-fly areas in the target area increase the overall path complexity, resulting in a change in the overall working time of the UAV. So in this algorithm, we respectively use the ''square wave signal'' curve for path planning at different base stations $S = S_0, S_1, S_2, S_3$ and calculate the overall working time of the UAV group by MBS-MUCCPPAFOA algorithm. The scheme with the shortest overall time consumption was selected as the final execution scheme for the MBS-MUCCPPAFOA algorithm. The UAV coverage path assignments are shown in Fig. 8. Pseudocode as in Algo. 2.

C. MULTI-UAV COOPERATIVE COVERAGE PATH PLANNING ALGORITHM WITH FLEXIBLE OBSTACLE AVOIDANCE CAPABILITY BASED ON AREA SEGMENTATION

In Section III-B, we take the work area as a whole to carry out path planning, and set up four fixed base stations $S = S_0, S_1, S_2, S_3$ to support the UAV group to complete the scanning coverage work cooperatively. In this section, we propose a Multi-UAV cooperative coverage path planning algorithm with flexible obstacle avoidance capability based on area segmentation called MUAV-CCPPAFOA-AS. The work area is divided into four regions: $Areas_{list} = \{a, b, c, d\}$ by region division, path planning is carried out for each region, and each base station corresponds to a single region for path planning and coverage search.

The work area was divided according to the following rules. The first area consists of all cells in column 1 through $column_{mid}$ and all cells in row 1 through row_{mid}. The second region consists of all cells in the columns $column_{mid}$ + 1 through m and all cells in row 1 through row_{mid}. The third

Algorithm 2 MBS-MUCCPPAFOA

Input: $Maxtim$, $\hat{P}$, $SPACE$, V, E, HT, S, $List_{src}$, SEL, $HTEL$, N
Output: P_{Drones}, t

```
L ← 0
U ← Maxtime
LP_Drones ← []
while True do
    t ← (L+U)/2
    P_Drones ← []
    for i = 1 to N do
        T_u ← t
        LP ← S
        P_u ← []
        j ← 0
        while True do
            C ← P̂[j]
            C_state Find the state of C in SPACE
            t_c ← dist(LP,C)/V
            if C_state is 0 then
                t_c ← dist(LP,C)/V +HT
            Select the nearest to the C from List_src as S
            t_b, List_b //time and path coordinates of C back to S
            if T_u ≥ t_c + t_r then
                t_u ← t_u − t_c
                C_state ← 1
                C append to P_u
                LP ← C
            else
                Add the path coordinates of LP back to S to P_u
                break
            j ← j + 1
        Remove the travelled point from P̂
        P̂[: 1] ← path coordinates of S move to C
    if 0 ∉ SPACE′ and LP_u ≥ P_u then
        U ← t
        LP_u ← P_u
    if 0 ∉ SPACE′ and LP_u = P_u then
        if ∀i ∈ {1, 2, ..., N}, Σ_{j=1}^{n} E_ij ≤ E then
            break
        U ← t
    if 0 ∈ SPACE′ then
        L ← t
return P_Drones, t
```

region consists of all cells in column 1 through $column_{mid}$ and in row $row_{mid}+1$ through n, and the remaining cells are the fourth region. $column_{mid}$ and row_{mid} can be obtained by:

$$column_{mid} = \begin{cases} m/2 & \text{m is even number} \\ m//2 & \text{m is odd number} \end{cases}$$
$$row_{mid} = \begin{cases} n/2 & \text{n is even number} \\ n//2 & \text{n is odd number} \end{cases} \quad (7)$$

We set two base stations in advance in the outer center position of each divided area belonging to the edge of the overall working area $BSlist = \{a : \{a_1, a_2\}, \ldots, d : \{d_1, d_2\}\}$, and use the "square wave signal" curve for path planning based on each area of the two base stations to

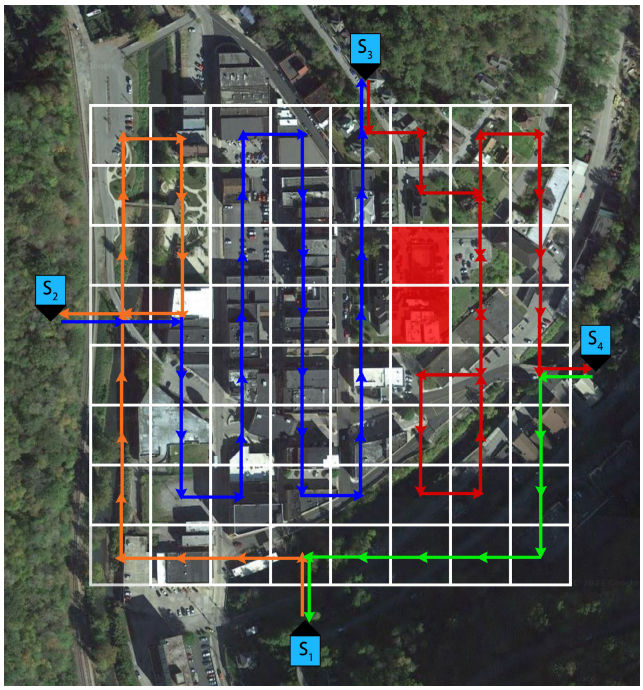

FIGURE 8. MBS-MUCCPPAFOA algorithm UAV coverage path assignment example diagram.

generate two working paths $Areas\hat{P}$: $\{a : \{a_1 : \hat{P}_{a_1}, a_2 : \hat{P}_{a_2}\}, \ldots, d : \{d_1 : \hat{P}_{d_1}, d_2 : \hat{P}_{d_2}\}\}$. The different locations of the obstacles or no-fly areas in each divided area may affect the working time of the entire working area. To find an unmanned path allocation scheme that reduces the overall working time of the UAV, similar to the working scheme of the overall target area, this study compared the path planning through the "square wave signal" curve algorithm at different base stations and the work allocation for each UAV through the MUAV-CCPPAFOA algorithm, and selected a group of schemes with the least overall time consumption as the final execution scheme of the UAV group. The UAV coverage path assignments are shown in Fig. 9. Pseudocode as in Algo. 3.

IV. PERFORMANCE EVALUATION

In this section we compare the performances of the proposed algorithm in detail. First, we describe the parameters and settings of the simulation scheme and then analyze the comparison results and evaluate the performance of the algorithm.

A. SIMULATION EXPERIMENTS AND RESULTS ANALYSIS UNDER DIFFERENT WORK AREA SIZES

To more clearly demonstrate the robustness of our proposed algorithm, we used the most common scanning coverage path planning algorithm with only one UAV base station as the baseline algorithm for comparison (as shown in Fig. 1(a)), and also provided the same obstacle avoidance ability. In this paper, we call this the Multi-UAV scanning coverage path planning algorithm (MUSCPP). In our research, the path based on the proposed Multi-UAV coverage path allocation

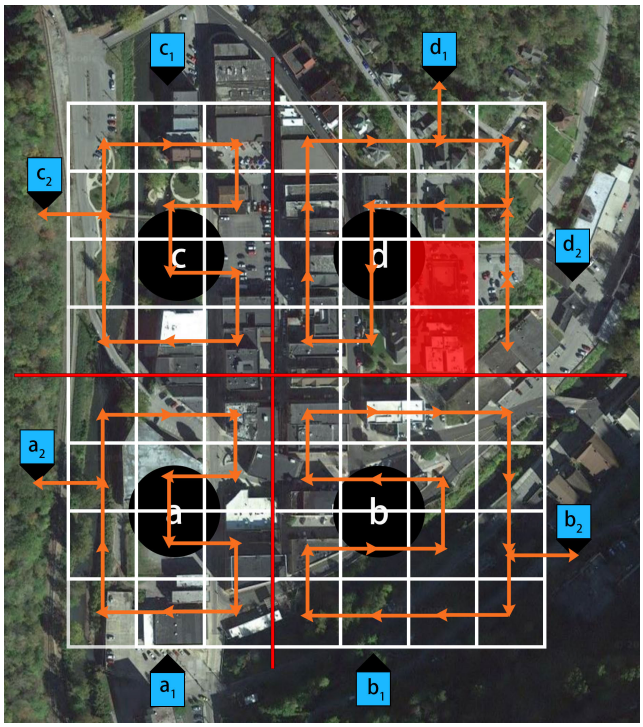

FIGURE 9. MUAV-CCPPAFOA-AS algorithm UAV coverage path assignment example diagram.

Algorithm 3 MUAV-CCPPAFOA-AS

Input: $Areas\hat{P}$, $SPACE$, V, E, HT, SEL, $HTEL$, N
Output: AllBestP, T

$Areas\hat{P}$: $\{a : \{a_1 : \hat{P}_{a_1}, a_2 : \hat{P}_{a_2}\}, \ldots, d : \{d_1 : \hat{P}_{d_1}, d_2 : \hat{P}_{d_2}\}\}$
$t_{max} \leftarrow 0$
$P_{Drones} \leftarrow []$
for $Area\hat{P} \in Areas\hat{P}.values()$ **do**
  $t_{min} \leftarrow \infty$
  for S, $\hat{P} \in Area\hat{P}.items()$ **do**
    $Maxtime \leftarrow$ Equation (5)
    DronesP, Time $\leftarrow$ Algo.1($Maxtime$, $\hat{P}$, $SPACE$, V, E, HT, S, SEL, $HTEL$, N)
    if Time $< t_{min}$ **then**
      $t_{min} \leftarrow$ Time
      BestP $\leftarrow$ DronesP
  if $t_{min} \geq t_{max}$ **then**
    $t_{max} \leftarrow t_{min}$
  BestP append to P_{Drones}
return P_{Drones}, t_{max}

algorithm is the "Square Wave Signal" curve path, and the "Square Wave Signal" curve path has four cases. To demonstrate the performance of the algorithm more comprehensively, we will show the four cases.

The working area size was set according to Table. 2. We set the number N of UAVS as 8, the initial energy E of UAVS as 100%, the flying speed V of UAUs as 5m/s, the energy consumption SEL as 0.110% per second when the speed is 5m/s, the coverage radius R of the camera sensor of UAVS as 25m, the hovering time HT of C area of each cell in the working area was set 1 second and the $HTEL$ of hovering time was 0.0757%. The number of areas with obstacles in the working area was defined as 10. We set the positions of obstacles in the work area to be randomly generated, simulated and tested 10 times for each work area size, and averaged the time for the UAV to complete the coverage of the entire work area.

Fig. 10, Fig. 11, Fig. 12 and Fig. 13 show the results of the simulation experiments. It can be easily found from the four figures that MBS-MUCCPPAFOA algorithm and MUAV-CCPPAFOA-AS algorithm with multiple base stations can significantly improve the robustness of multiple UAVS to perform coverage tasks. Fig. 11 and Fig. 12 show the test results for a working area with the same area but different aspect ratios. From the results, the performance of the MUSCPP and MUAV-CCPPAFOA algorithms with only one base station is significantly affected by the change in the division of the cell area in the working area, whereas the performance of the MBS-MUCCPPAFOA and MUAV-CCPPAFOA-AS algorithms is less affected. Fig. 10, Fig. 11 and Fig. 12, it is not difficult to find that the performance of MUAV-CCPPAFOA-AS algorithm is always stronger than that of MBS-MUCCPPAFOA algorithm. In Fig. 13, we can see that the performance of algorithm B is still better than that of algorithm A when the working area is $750m \times 750m$ and $850m \times 850m$, but the performance of algorithm B is slightly inferior to that of algorithm A when the working area is $650m \times 650m$ and $950m \times 950m$. When the working area was $950m \times 950m$, the MUSCPP algorithm could not complete the coverage task of the working area under the same parameters as the other algorithms.

B. SIMULATION EXPERIMENTS AND RESULTS ANALYSIS OF DIFFERENT ENVIRONMENTAL COMPLEXITY IN THE WORKING AREA

To evaluate the performance of the algorithm for different complexities of the working environment, we set the number of obstacles in the working area to 5, 10, 15 and 20, respectively. The working area is set to meet the four cases of the square wave signal curve path: $800m \times 800m$, $800m \times 850m$, $850m \times 800m$, and $850m \times 850m$. We let the positions of the obstacles be randomly generated and simulated 10 times for different numbers of obstacles. The other parameters were consistent with those in SectionIV-A.

In view of Fig. 13, we observed the results of ten simulation experiments in detail. Because the MUAV-CCPPAFOA-AS algorithm divided the area into four sub-areas, and then carried out UAV coverage search work, and the position of obstacles was randomly generated, it was possible that obstacles were concentrated in a certain sub-area, resulting in a much higher environmental complexity in this area than in other sub-areas, resulting in a longer overall work.

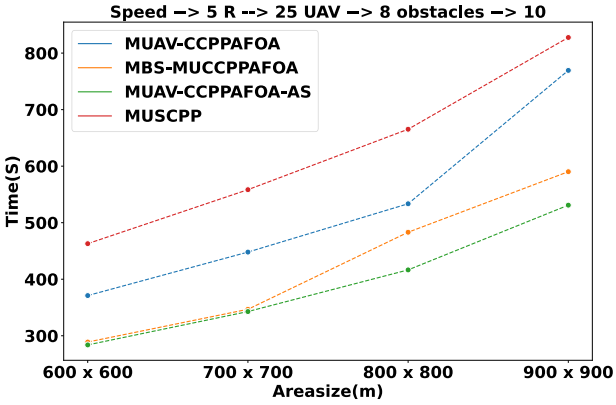

FIGURE 10. Work area divided into even rows and columns.

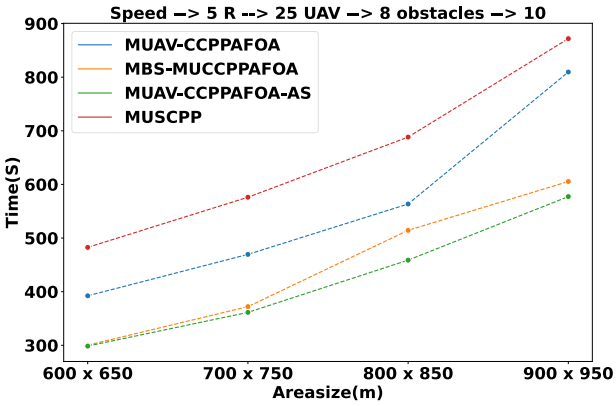

FIGURE 11. Work area divided into even columns and odd rows.

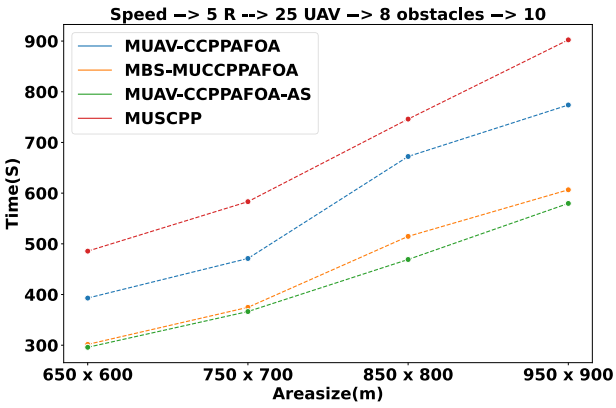

FIGURE 12. Work area divided into odd columns and even rows.

To accurately and stably show the discrete distribution of experimental results in different complexity working areas, we used box plots to show the results of the simulation experiments. Fig. 14, Fig. 15, Fig. 16 and Fig. 17 show the results of simulation experiments.

The upper quartile of the box plots in our figure was set to 90% and the lower quartile was set to 5%. It is evident from the four figures that the path of the UAV in the region is somewhat impacted by the number of obstacles present, and that all algorithms experience a slight increase in working time. The MBS-MUCCPPAFOA algorithm exhibited the least amount of performance

TABLE 2. Area size.

Type of work area	Working area length and width	Unit
Even columns and even rows:	$600 \times 600, 700 \times 700, 800 \times 800, 900 \times 900$	m
Even columns and odd rows:	$600 \times 650, 700 \times 750, 800 \times 850, 900 \times 950$	m
Odd columns and even rows:	$650 \times 600, 750 \times 700, 850 \times 800, 950 \times 900$	m
Odd columns and odd rows:	$650 \times 650, 750 \times 750, 850 \times 850, 950 \times 950$	m

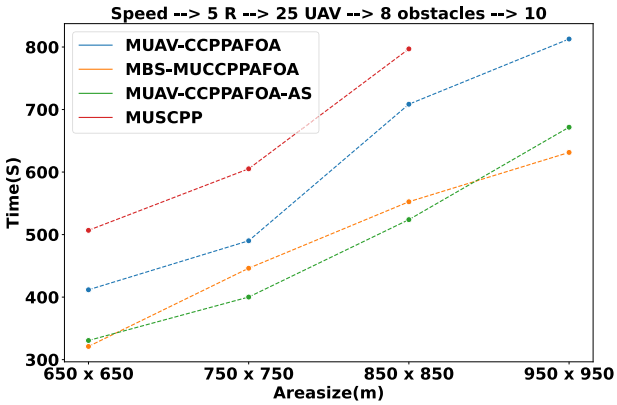

FIGURE 13. Work area divided into odd columns and rows.

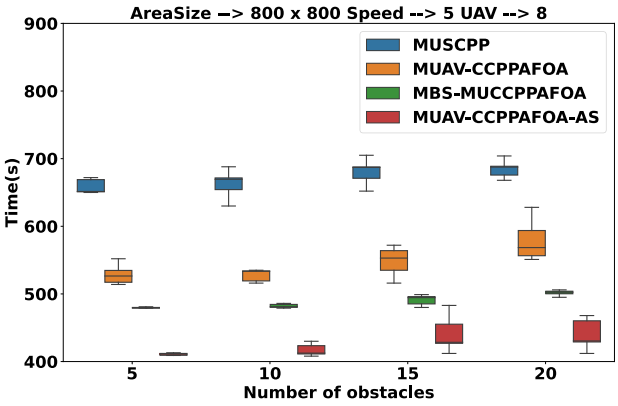

FIGURE 14. Work area divided into even rows and columns(800 × 800).

variation; however, the obstacle position factor had an impact on the MUAV-CCPPAFOA and MUAV-CCPPAFOA-AS algorithms. In addition, there was a noticeable variance in the time required to cover the entire work area. The overall performance of the MUAV-CCPPAFOA-AS algorithm is much stronger than that of the MBS-MUCCPPAFOA algorithm, despite the noticeable oscillations in the time it takes to cover the entire work area. In additionally, we observed that the MUAV-CCPPAFOA-AS algorithm outperformed the MBS-MUCCPPAFOA method, which in turn outperformed the MUAV-CCPPAFOA algorithm in terms of algorithm performance.

In the simulation test, we find that when the work area to be detected is small and the obstacles (no-fly area) are more and more concentrated, the overall working time of MUAV-CCPPAFOA-AS algorithm will be longer because the work complexity of a certain division area is much higher

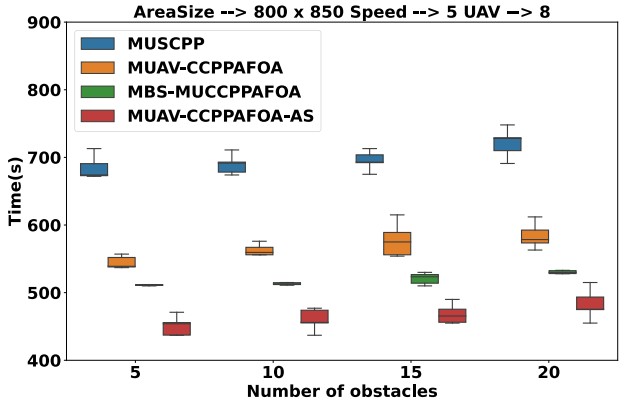

FIGURE 15. Work area divided into even columns and odd rows(800 × 850).

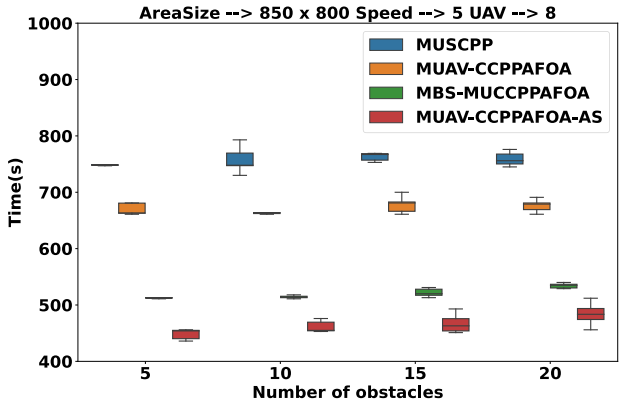

FIGURE 16. Work area divided into odd columns and even rows(850 × 800).

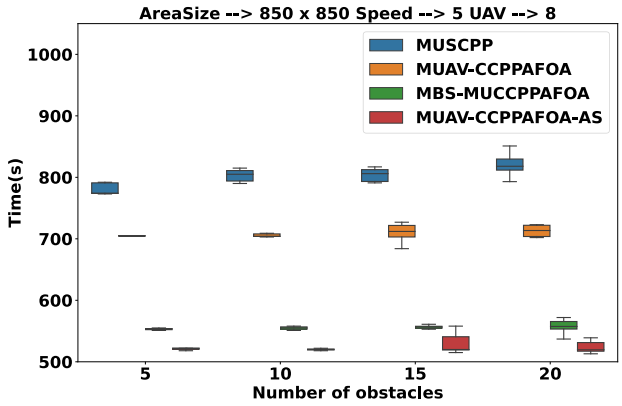

FIGURE 17. Work area divided into odd columns and rows(850 × 850).

than that of other division areas, and the performance of MUAV-CCPPAFOA-AS algorithm will be longer It is slightly lower than MBS-MUCCPPAFOA algorithm. However, this situation will gradually reduce the impact on the performance of the MUAV-CCPPAFOA-AS algorithm with an increase in the working area. In other cases, MUAV-CCPPAFOA-AS performed better than MBS-MUCCPPAFOA.

V. CONCLUSION

In this study, for the regional coverage path planning problem, we propose two cooperative coverage path planning algorithms for multiple UAVs with multiple base stations, namely the MBS-MUCCPPAFOA and MUAV-CCPPAFOA-AS algorithms. The aim is to reduce the amount of energy and time wasted by the UAV in the process of moving to the area where the task is assigned. The MBS-MUCCPPAFOA algorithm plans the path of the work area as a whole, and then covers the entire area through the cooperation of multiple UAVs. In the MUAV-CCPPAFOA-AS algorithm, the work area is divided into four regions, and path planning is performed for each sub-region. Multiple UAVs cooperate to cover and search each sub-region to achieve the purpose of cover and search the entire region.

Through extensive simulations, we demonstrate that multiple base stations can significantly improve the performance of the Multi-UAV cooperative coverage path planning algorithm. Through detailed a evaluation, we demonstrate that the MUAV-CCPPAFOA-AS algorithm can reduce the time required to complete the coverage search of the entire work area.

REFERENCES

[1] L. Abualigah, A. Diabat, P. Sumari, and A. H. Gandomi, "Applications, deployments, and integration of Internet of Drones (IoD): A review," *IEEE Sensors J.*, vol. 21, no. 22, pp. 25532–25546, Nov. 2021.

[2] S. Yan, C.-S. Sun, and Y.-H. Chen, "Optimal routing and scheduling of unmanned aerial vehicles for delivery services," *Transp. Lett.*, vol. 15, pp. 1–12, Jul. 2023.

[3] S. M. S. M. Daud, M. Y. P. M. Yusof, C. C. Heo, L. S. Khoo, M. K. C. Singh, M. S. Mahmood, and H. Nawawi, "Applications of drone in disaster management: A scoping review," *Sci. Justice*, vol. 62, no. 1, pp. 30–42, 2022.

[4] A. Nedjati, G. Izbirak, B. Vizvari, and J. Arkat, "Complete coverage path planning for a multi-UAV response system in post-Earthquake assessment," *Robotics*, vol. 5, no. 4, p. 26, 2016.

[5] J. Shahmoradi, E. Talebi, P. Roghanchi, and M. Hassanalian, "A comprehensive review of applications of drone technology in the mining industry," *Drones*, vol. 4, no. 3, p. 34, Jul. 2020.

[6] H. Madjidi, S. Negahdaripour, and E. Bandari, "Vision-based positioning and terrain mapping by global alignment for UAVs," in *Proc. IEEE Conf. Adv. Video Signal Based Surveill.*, Jul. 2003, pp. 305–312.

[7] X. Lyu, X. Li, D. Dang, H. Dou, K. Wang, and A. Lou, "Unmanned aerial vehicle (UAV) remote sensing in grassland ecosystem monitoring: A systematic review," *Remote Sens.*, vol. 14, no. 5, p. 1096, Feb. 2022.

[8] T. Oksanen and A. Visala, "Coverage path planning algorithms for agricultural field machines," *J. Field Robot.*, vol. 26, no. 8, pp. 651–668, Aug. 2009.

[9] E. Yanmaz, "Joint or decoupled optimization: Multi-UAV path planning for search and rescue," *Ad Hoc Netw.*, vol. 138, Jan. 2023, Art. no. 103018.

[10] W. Wang, L. Zhang, J. Li, X. Yuan, Y. Shi, Q. Jiang, and L. He, "The force control and path planning of electromagnetic induction-based massage robot," *Technol. Health Care*, vol. 25, pp. 275–285, Jul. 2017.

[11] X. Miao, H.-S. Lee, and B.-Y. Kang, "Extended BSA coverage algorithm for large unknown map," *J. Korean Inst. Intell. Syst.*, vol. 27, no. 5, pp. 408–419, Oct. 2017.

[12] A. Sans-Muntadas, E. Kelasidi, K. Y. Pettersen, and E. Brekke, "Spiral path planning for docking of underactuated vehicles with limited FOV," in *Proc. IEEE Conf. Control Technol. Appl. (CCTA)*, Aug. 2017, pp. 732–739.

[13] T. M. Cabreira, C. D. Franco, P. R. Ferreira, and G. C. Buttazzo, "Energy-aware spiral coverage path planning for UAV photogrammetric applications," *IEEE Robot. Autom. Lett.*, vol. 3, no. 4, pp. 3662–3668, Oct. 2018.

[14] H. Moravec and A. Elfes, "High resolution maps from wide angle sonar," in *Proc. IEEE Int. Conf. Robot. Autom.*, Mar. 1985, pp. 116–121.

[15] H. Choset, "Coverage for robotics—A survey of recent results," *Ann. Math. Artif. Intell.*, vol. 31, pp. 113–126, Oct. 2001.

[16] K. Sandamurthy and K. Ramanujam, "A survey on coverage path planning algorithms for autonomous robots in agriculture," *Int. J. Comput. Sci. Eng.*, vol. 7, no. 3, pp. 815–827, Mar. 2019. [Online]. Available: https://www.ijcseonline.org/full_paper_view.php?paper_id=3923
[17] M. Alharbi and H. A. Karimi, "A global path planner for safe navigation of autonomous vehicles in uncertain environments," *Sensors*, vol. 20, no. 21, p. 6103, Oct. 2020.
[18] J. Shi and M. Zhou, "A data-driven intermittent online coverage path planning method for AUV-based bathymetric mapping," *Appl. Sci.*, vol. 10, no. 19, p. 6688, Sep. 2020.
[19] C. C. Murray and A. G. Chu, "The flying sidekick traveling salesman problem: Optimization of drone-assisted parcel delivery," *Transp. Res. C, Emerg. Technol.*, vol. 54, pp. 86–109, May 2015.
[20] T. Cabreira, L. Brisolara, and P. R. Ferreira, "Survey on coverage path planning with unmanned aerial vehicles," *Drones*, vol. 3, no. 1, p. 4, Jan. 2019.
[21] Z. Zhen, D. Xing, and C. Gao, "Cooperative search-attack mission planning for multi-UAV based on intelligent self-organized algorithm," *Aerosp. Sci. Technol.*, vol. 76, pp. 402–411, May 2018.
[22] Y. Hou, X. Liang, L. He, and L. Liu, "Cooperative area search algorithm for uav swarm in unknown environment," *J. Beijing Univ. Aeronaut. Astronaut.*, vol. 45, no. 2, p. 347, 2019.
[23] A. V. Le, N. H. K. Nhan, and R. E. Mohan, "Evolutionary algorithm-based complete coverage path planning for tetriamond tiling robots," *Sensors*, vol. 20, no. 2, p. 445, Jan. 2020.
[24] M. Kloetzer, C. Mahulea, and R. Gonzalez, "Optimizing cell decomposition path planning for mobile robots using different metrics," in *Proc. Int. Conf. Syst. Theory, Control Comput.*, Cheile Gradistei, Romania, Oct. 2015, pp. 565–570.
[25] K. Li and Y. Chen, "A full coverage path planning algorithm based on backtracking method," *Comput. Eng. Sci.*, vol. 41, no. 7, p. 1227, 2019.
[26] J. Liang, B. Zeng, and Y. He, "Research on path planning algorithm for cleaning robot based on improved potential field grid method," *J. Guangdong Univ. Technol.*, vol. 33, no. 4, pp. 30–36, 2016.
[27] Z. Huinan, M. Lei, S. Hui, and J. Baohua, "A study on full-coverage path planning for mobile robots," *Comput. Simul.*, vol. 36, no. 3, pp. 298–301, 2019.
[28] Y. Yu and S. Lee, "Efficient multi-UAV path planning for collaborative area search operations," *Appl. Sci.*, vol. 13, no. 15, p. 8728, Jul. 2023.

YANG YU received the B.S. degree in computer engineering from Qingdao University, Qingdao, China, in 2018, and the M.S. degree in computer science from Kookmin University, Seoul, Republic of Korea, in 2021, where he is currently pursuing the Ph.D. degree in computer science. His current research interests include remote driving, the Internet of Things (IoT), coverage path planning, UAV, and video streaming.

SANGHWAN LEE received the B.S. and M.S. degrees from Seoul National University, South Korea, in 1993 and 1995, respectively, and the Ph.D. degree from the Department of Computer Science and Engineering, University of Minnesota, in September 2005. After earning the M.S. degree, he was with Hyundai Electronics, South Korea, for five years. He joined the Department of Computer Science and Engineering, University of Minnesota, in fall 2000. From June 2005 to February 2006, he was with the IBM T. J. Watson Research. He joined Kookmin University, Seoul, South Korea, in March 2006. His main research interests include software-defined networking (SDN), scalable routing selection for multimedia, and various theories and services needed on the internet.